

Original Article

High-throughput sequencing analysis of the expression profile of microRNAs and target genes in mechanical force-induced osteoblastic/cementoblastic differentiation of human periodontal ligament cells

Yun Wu^{1,2}, Yanjing Ou^{1,2}, Chufang Liao^{1,2}, Shanshan Liang^{1,2}, Yining Wang^{1,2}

¹The State Key Laboratory Breeding Base of Basic Science of Stomatology (Hubei-MOST) and The Key Laboratory of Oral Biomedicine Ministry of Education, School and Hospital of Stomatology, Wuhan University, Wuhan, PR China; ²Department of Prosthodontics, Hospital of Stomatology, Wuhan University, Wuhan, PR China

Received December 29, 2018; Accepted May 6, 2019; Epub June 15, 2019; Published June 30, 2019

Abstract: Mechanical tension force directs the lineage commitment of periodontal ligament cells (PDLs) to osteogenesis; however, the underlying mechanisms, especially those at the post-transcriptional level, remain unclear. In the present study, we developed an in vitro force-loading model for PDLs. Then, high-throughput sequencing was used to identify the expression profile of microRNAs (miRNAs) for stretched PDLs. The candidate target genes of differentially expressed miRNAs were predicted by bioinformatics analysis. A total of 47 miRNAs were found to be differentially expressed in stretched and non-stretched PDLs; of these, 31 were upregulated and 16 were downregulated. Further, 9 osteogenesis-related miRNAs (miR-221-3p, miR-138-5p, miR-132-3p, miR-218-5p, miR-133a-3p, miR-145-3p, miR-143-5p, miR-486-3p, and miR-21-3p) were validated by quantitative reverse transcription-polymerase chain reaction (RT-qPCR). Gene Ontology (GO) and Kyoto Encyclopedia of Gene and Genome (KEGG) pathway analysis were then carried out to reveal the potential functions of predicted target genes. Among the top 20 enriched pathways, the Hippo signaling pathway was selected for further functional analysis. Several important components of the Hippo signaling pathway, including YAP1, WWTR1, TEAD2, CTGF, DVL2, GDF5, GLI2, LIMD1, WTIP, LATS1, and TEAD1, were predicted to be target genes of differentially expressed miRNAs and were determined to be upregulated in stretched PDLs. Among them, YAP1, WWTR1, TEAD2, CTGF, DVL2, and GDF5 were positive regulators of osteogenesis. These findings may provide a reliable reference for future studies to elucidate the biological mechanisms of orthodontic tooth movement (OTM).

Keywords: Periodontal ligament cells, osteogenesis, high-throughput sequencing, microRNA, orthodontic tooth movement

Introduction

Orthodontic tooth movement (OTM) relies on coordinated tissue resorption and formation in the surrounding bone and periodontal ligament. The periodontal ligament (PDL) is a dense fibrous connective tissue structure consisting of collagenous fiber bundles, cells, neural and vascular components, and tissue fluids [1]. Its primary function is to support the teeth in their sockets while allowing the teeth to withstand considerable chewing forces. The PDL acts as an important medium, transducing the mechanical force from the teeth to the alveolar bone, and then transferring it into biochemical

signals [2, 3]. Bone formation and resorption happens at the tension side and compressive side, respectively [4]. To date, the underlying mechanisms by which the PDL perceives mechanical loading and initiates the process of bone remodeling have not yet been fully elucidated.

PDL cells (PDLs), a heterogeneous cell population within the PDL, are considered to be the first cellular recipients of mechanical stimuli. Previous studies have demonstrated that PDLs possess a portion of mesenchymal stem cells, which can further differentiate to an osteoblastic and cementoblastic phenotype and

involve in the alveolar bone and root cementum remodeling process during the orthodontic tooth treatment [5-7]. Besides, it was shown that multiple regulators, including cytokines, growth factors, cytoskeleton proteins, and signaling pathways (e.g., ERK1/2, p38 mitogen-activated protein kinases (MAPK) signaling pathway, ephrin B2/EphB4 signaling) are involved in the modulation of the osteogenic activities of PDLs under mechanical stimuli [8-10]. Recently, another regulatory mechanism involved in osteoblastic/cementoblastic differentiation of PDLs after mechanical force loading have been reported to be post-transcriptional modulation of gene expression by microRNAs (miRNAs).

miRNAs are short non-coding RNAs composed of approximately 22 nucleotides; they regulate gene expression by selectively binding to the 3' untranslated regions (3'-UTR) of target mRNAs, resulting in mRNA degradation or protein translation repression [11, 12]. In recent years, increasing evidence has indicated that miRNAs are involved in the cellular response to various mechanical stimuli in diverse organs and cells. Among them, miR-33-5p was identified as a novel mechano-sensitive miRNA that positively regulates osteoblast differentiation by repressing the expression of high mobility group AT-hook 2 (Hmga2) [13]. Additionally, miR-503-5p is reported to function as a mechano-responsive miRNA which can inhibit osteogenic differentiation of bone marrow-derived mesenchymal stem cells (BMSCs) subjected to mechanical stretch and bone formation in OTM tension sides [14]. Under tensile stress, miR-154-5p was found to negatively regulate osteogenic differentiation of adipose tissue-derived stem cells (ADSCs) through the Wnt/planar cell polarity (PCP) signaling pathway by directly targeting Wnt11 [15]. In addition, miRNAs also participate in osteogenesis of PDLs under mechanical loading. Previous studies have shown that miR-132 regulates the osteogenic differentiation of PDLs after fluid shear stress treatment through the mTOR signaling pathway [16]. Of note, miR-21 has been reported to play a role in osteogenic differentiation of PDLs exposed to stretch in vitro, and can modulate OTM and alveolar bone remodeling in the presence of both normal and inflammatory microenvironments in vivo [17, 18]. Further, miR-195-5p was found to be downregulated and nega-

tively correlated with osteogenic differentiation of PDLs under cyclic tension straining for 72 hours [19]. Although several miRNAs have been identified to play a role in stretch-induced osteogenic differentiation of PDLs, the functional roles and regulatory mechanisms of miRNAs during osteogenesis and bone formation under force-loading have not been fully explored.

High-throughput sequencing techniques have been successfully used to identify miRNAs in a variety of organisms. Compared with microarray assay, next-generation sequencing allows deep sequencing in a short period of time, and has been able to identify new, previously unreported miRNAs [20]. In the present study, to further clarify the regulatory effect of miRNAs in osteoblastic/cementoblastic differentiation of stretched PDLs, we examined differentially expressed miRNAs in stretched PDLs and non-stretched PDLs using high-throughput sequencing. Relative target genes of differentially expressed miRNAs were also predicted using bioinformatics analysis. Then, these putative target genes were analyzed by Gene Ontology (GO) and Kyoto Encyclopedia of Genes and Genomes (KEGG) pathway analyses. Additionally, the interaction between osteogenesis-related transcription factors and changed miRNAs was predicted using bioinformatics tools in order to investigate osteoblastic/cementoblastic mechanisms of PDLs under force loading.

Materials and methods

Cell culture

Healthy third molar teeth were collected in a clinical setting from individuals aged 14-25 years. Informed consent was obtained from all participants and the study protocol was approved by the Ethics Committee, School of Stomatology, Wuhan University, Wuhan, China. Human PDLs were obtained from human tissue scraped from the roots of the extracted teeth. In brief, extracted teeth were rinsed three times with phosphate-buffered saline (PBS) containing 10% penicillin and streptomycin. Tissue was obtained from the middle one-third of the roots, and was placed into a 25 cm² tissue culture flask containing α -modified essential medium (α -MEM; HyClone, Logan, UT, USA) supplemented with 20% fetal bovine serum (FBS; HyClone, Logan, UT, USA), 100 U/mL penicillin G, and 100 μ g/mL streptomycin.

miRNAs and osteoblastic/cementoblastic differentiation of PDLCs

The explants were incubated at 37°C with 5% CO₂. When sub-confluence was reached, PDLCs were passaged; cells at passages 3-6 were used for the following experiments.

Flow cytometry analysis

To identify the phenotype of PDLCs, cell surface markers were evaluated by flow cytometry. Briefly, a total of 1×10^6 cells were collected and incubated with FITC-labeled anti-CD146 antibodies (Biolegend, San Diego, California), anti-CD90 antibodies (Biolegend, San Diego, California), or anti-CD45 antibodies (Biolegend, San Diego, California) for 30 min at 4°C. Then, cells were washed three times with PBS and analyzed by flow cytometry analysis. The results were analyzed with FlowJo software (Tree Star, Ashland, OR, USA).

Osteoblast and adipocyte differentiation

PDLCs were seeded in six-well plates at a density of 1×10^5 per well. After reaching 70-80% confluence, cells were incubated with osteogenic medium containing 50 µg/ml ascorbic acid, 10 mmol/L β-glycerophosphate, and 10 nmol/L dexamethasone. The medium was changed every three days. After osteogenic induction for 7 days and 21 days, extracellular matrix calcification was investigated with alkaline phosphatase (ALP) staining with a BCIP/NBT kit (Beyotime, China) and Alizarin red staining, respectively.

For adipocyte differentiation, PDLCs were cultured in adipogenic medium, according to the manufacturer's instructions (Cyagen, Suzhou, China). Two weeks later, Oil Red O staining was used to detect lipid formation.

Application of tension force system

External mechanical stimulation was achieved with a Flexcell FX-5000™ tension system (Flexcell International Corp., Burlington, NC, USA). PDLCs were plated onto six-well Bioflex plates coated with type I collagen (Flexcell International Corp., Burlington, NC, USA) at a density of approximately 1×10^5 cells/well. When the culture reached 70%-80% confluence, they were stretched with 10% equibiaxial strain at 0.1 Hz for 24 h in a Flexcell FX-5000™ tension system (Flexcell International Corp., Burlington, NC, USA). The control cells were cultured without stretching.

Western blot analysis

For Western blot analysis, cell lysates were prepared with radio-immunoprecipitation assay (RIPA) lysis buffer supplemented with phenylmethylsulfonyl fluoride (PMSF) (Roche, Germany) and phosphatase inhibitor (Roche, Germany). The samples were separated on a 10% sodium dodecyl sulfate polyacrylamide gel electrophoresis (SDS-PAGE), and transferred onto 0.22 µm polyvinylidene difluoride (PVDF) membranes. The membranes were blocked with 5% non-fat milk for 1 h at room temperature. Subsequently, these membranes were incubated with primary antibodies, including rabbit anti-runt-related transcription 2 (RUNX2) (1:500; Abclonal, Boston, MA), rabbit anti-secreted phosphoprotein 1 (SPP1) (1:1000; Abclonal, Boston, MA), rabbit anti-cementoblastoma-derived protein 1 (CEMP1) (1:500; Abcam, Cambridge, UK), and mouse anti-glyceraldehyde 3-phosphate dehydrogenase (GAPDH) (1:5000; Abcam, Cambridge, UK) monoclonal antibody, overnight at 4°C. Membranes were then washed three times with TBST and incubated with horseradish peroxidase (HRP)-conjugated secondary antibody for 1 h at room temperature. Immuno-reactive bands were detected using an enhanced chemiluminescence (ECL) kit, and were quantitatively analyzed with Image J software. GAPDH was used as the internal control.

DNA library construction and high-throughput sequencing

Total RNA was isolated from the two groups of cells (normal PDLCs and PDLCs stretched for 24 h), according to the manufacturer's instructions. RNA molecules sized 18-30 nt were enriched by PAGE. Then, the 3' and 5' adapters were ligated to the RNAs. The ligation products were constructed by reverse transcription polymerase chain reaction (RT-PCR), and PCR products sized 140-160 bp were enriched to generate a cDNA library and sequence using Illumina HiSeq™2500 (Illumina, Inc., San Diego, CA, USA).

Alignment and identification of miRNAs

Reads obtained from the sequencing machines were further filtered to achieve clean tags. All the clean tags were aligned with small RNAs using the GenBank 209 and Rfam11.0 data-

miRNAs and osteoblastic/cementoblastic differentiation of PDLs

Table 1. Primer sequences for RT-qPCR

Gene	Forward primer (5'-3')	Reverse primer (5'-3')
ALP	CGAGATACAAGCACTCCCACTTC	CTGTTCCAGCTCGTACTGCATGTC
BSP	CAGGGCAGTAGTGACTCATCC	TAGCCCAGTGTGTAGCAGA
COL1A1	CGATGGATTCCAGTTCGAG	TAGGTGATGTTCTGGGAGGC
SPP1	GTGGCCACATGGCTAAACCCT	GACTTACTTGGGAAGGGTCTGTGG
OCN	GGTGCAGCCTTTGTGTCCAA	CCTGAAAGCCGATGTGGTCA
RUNX2	AACCCTTAATTTGCACTGGGTCA	CAAATTCAGCAATGTTTGTGCTAC
CAP	CTGCGCGTGCACATGG	GCGATGTCGTAGAAGGTGAGCC
CEMP1	GGGCACATCAAGCACTGACAG	CCCTTAGGAAGTGGCTGTCCAG
SATB2	GCCCTGGTCTTCTTTCTCCC	CGGAAGAGTTGGTTGGCTCT
MSX2	GCCTCGGTCAAGTCGGAAAA	CGGCGCGCACTCACTT
TEAD1	CCATCCAGGGTTTGAGCCT	GCTTGGTTGTGCCAATGGAG
YAP1	TCCAGATGAACGTCACAGC	TCATGGCAAACGAGGGTCA
LATS1	TGAAGAGCGAAGGGAATCTCG	TTTAAAAGGTTTTACCCGCATCA
WTIP	CCACCTACTGTGTCGTCGTT	TCAGAGCTCAGTGACGTGC
GLI2	GCAGGTGTATCCCACGGAAA	CTGGCATCCTCCCAGCATAG
GDF5	GACTCCCCAAACTCCTCACTT	CACCCAACACAGTGCAGATGA
DVL2	AGTGAGCATGGCGCTGG	TCGCTGGTCATGAGGGTAGA
CTGF	GTTTGGCCAGACCCAATA	GGCTCTGCTTCTCTAGCCTG
LIMD1	GAGAGATGGATGCTACCCG	GTAGAGTTCCCCATGGCCT
WWTR1	TGGACCAAGTACATGAACCACC	GACTGGTGATTGGACACGGT
TEAD2	CCCCATCTACTGACCTCCCA	GTTCCACGAAGGCTGAGAA
GAPDH	AACAGCGACACCCACTCCTC	CATACCAGGAAATGAGCTTGACAA

bases to identify and remove rRNA, scRNA, snoRNA, snRNA, and tRNA. Meanwhile, the clean tags were aligned with the reference genome, and those mapped to exons, introns, and repeat sequences were also removed. Then, the clean tags were searched against miRBase21 to identify known miRNAs. All unannotated tags were aligned with the reference genome. Novel miRNA candidates were identified according to their genome positions and hairpin structures as predicted by Mireap v0.2 software.

Analysis of differentially expressed miRNAs

miRNAs with a fold change ≥ 2 and a *P*-value < 0.05 were considered to be significantly differentially expressed.

Prediction of miRNA target genes and functional enrichment analysis

Based on the differential expression profile of miRNAs, the candidate target genes were predicted using three software programs (RNAhybrid v. 2.1.2 + svm-light v. 6.01, Miranda v. 3.3a, and TargetScan v. 7.0). The intersection of the results was chosen as the predicted

miRNA target genes. GO terms and KEGG pathway annotation were used to further identify the biological functions of the target genes. Genes with a false discovery rate (FDR) < 0.05 were considered to be significantly enriched target candidate genes.

Quantitative RT-PCR (RT-qPCR)

To measure the mRNA level of miRNAs and other genes, total RNA was isolated from PDLs and rat periodontal ligament tissue using a mirVana™ miRNA isolation kit (Invitrogen, Carlsbad, CA, USA). Then, 1 μ g of total RNA was reverse-transcribed using a Mir-X miRNA First-Strand Synthesis kit and PrimerScript RT Reagent kit with gDNA Eraser (Takara, Tokyo, Japan). SYBR Premix Ex Taq II (Takara, Tokyo, Japan) was used for RT-qPCR analy-

sis, according to the manufacturer's instructions. The relative expression of mRNA or miRNA was calculated using the $2^{-\Delta\Delta Ct}$ method and normalized to the expression of GAPDH or U6, respectively. All PCRs were performed in triplicate. The miRNA primer sets were purchased from GenePharma (Suzhou, China). And the primer pairs of the relative genes are shown in **Table 1**.

OTM

Twelve eight-week-old male Wistar rats weighing 180 to 220 g were used in this study. All procedures involving animals were performed in accordance with the ethical standards of our institution, and were approved by the Institutional Animal Care and Use Committee of Wuhan University. In brief, we used a 0.2 mm nickel-titanium coil spring (TOMY International Inc., Tokyo, Japan) to connect the maxillary left first molar to the incisors. A tension gauge was utilized to calculate the force magnitude in the stretch direction. The non-stretched right upper first molars with no appliance acted as the corresponding control. For each condition in our experiment, six animals were used at each time point. After 3 days, the PDL tissue from each

miRNAs and osteoblastic/cementoblastic differentiation of PDLs

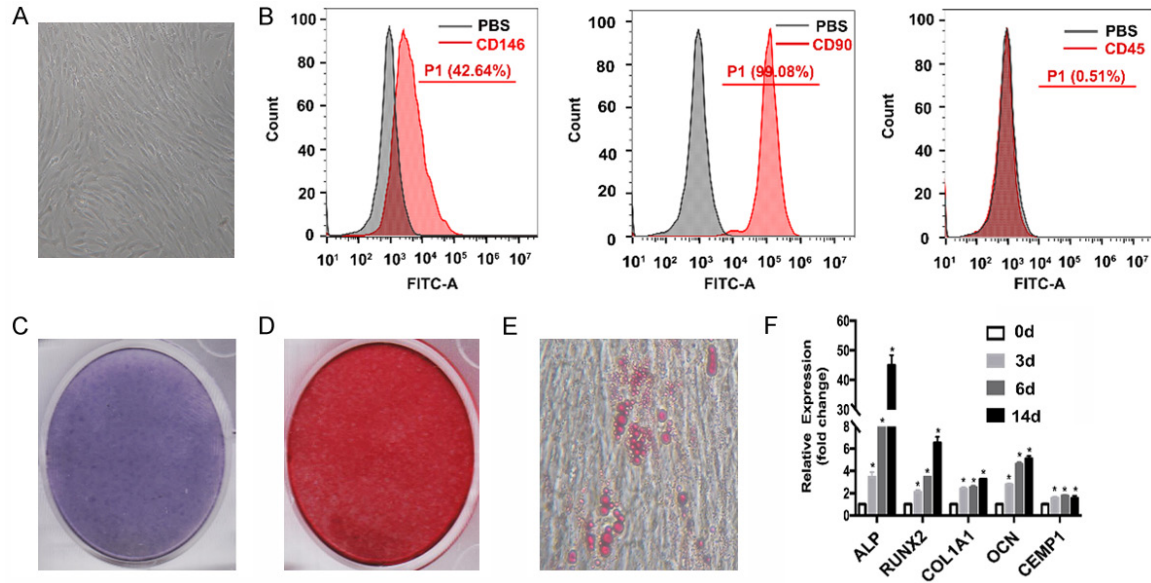


Figure 1. Morphology and characterization of human periodontal ligament cells (PDLs). (A) Cultured single cells grew to confluence in two weeks, exhibiting spindle, fibroblast-like morphology. (B) Flow cytometry analysis indicated that cultured PDLs were positive for mesenchymal stem cell markers CD146 (42.64%) and CD90 (99.08%), and negative for CD45 (0.51%). (C) ALP and (D) Alizarin red staining indicated the presence of calcium deposits and mineralized nodules in PDLs after osteogenic induction for 7 days and 21 days, respectively. (E) Lipid accumulation was detected by Oil Red O staining of PDLs cultured for 14 days with adipogenic medium. (F) Relative expression levels of the osteogenic/cementoblastic markers ALP, RUNX2, COL1A1, OCN and CEMP1 were upregulated during the process of osteogenesis of PDLs ($P < 0.05$). * $P < 0.05$ vs. control.

rat's distal stretched side and the control side was collected for RT-qPCR analysis.

Measurement of OTM

Rats were sacrificed 14 days after orthodontic force application. The maxillary alveolar bone together with three molars on the right and left sides were isolated and submitted to X-ray photography (Bruker Corp., Billerica, MA, USA). Mesial molar movement was determined by the distance between the cemento-enamel junctions of the orthodontic loaded first molars and the second molars. The measurement of OTM was performed using the ruler tool in Adobe Photoshop software (Adobe Inc., San Jose, CA, USA).

Hematoxylin and eosin (H&E) staining

The maxillary alveolar bone and the three molars from each rat were fixed with 4% paraformaldehyde for 24 h at room temperature. They were then decalcified for 3 months using 10% EDTA (pH = 7.4) and then dehydrated and embedded in paraffin. All specimens were cut into 5 μ m sections and were then deparaffinized and rehydrated. H&E staining was per-

formed for histological and histomorphometric analysis.

Statistical analysis

Statistical analysis was undertaken by SPSS 16.0 software (IBM, Armonk, NY, USA) or GraphPad Prism 5.0 software. All quantitative data were presented as mean \pm standard deviation (SD) of at least three independent experiments. Statistical difference was assessed by student's t test or one-way analysis of variance (ANOVA) in either two or multiple groups. A P -value < 0.05 was considered statistically significant.

Results

Morphology and characterization of PDLs

PDLs derived from periodontal ligament tissue reached confluence in two weeks, exhibiting spindle, fibroblast-like morphology (**Figure 1A**). Flow cytometry analysis indicated that cultured PDLs were positive for mesenchymal stem cell markers (CD146, CD90) and negative for CD45 (**Figure 1B**). ALP and alizarin red staining revealed calcium deposits and mineralized

miRNAs and osteoblastic/cementoblastic differentiation of PDLs

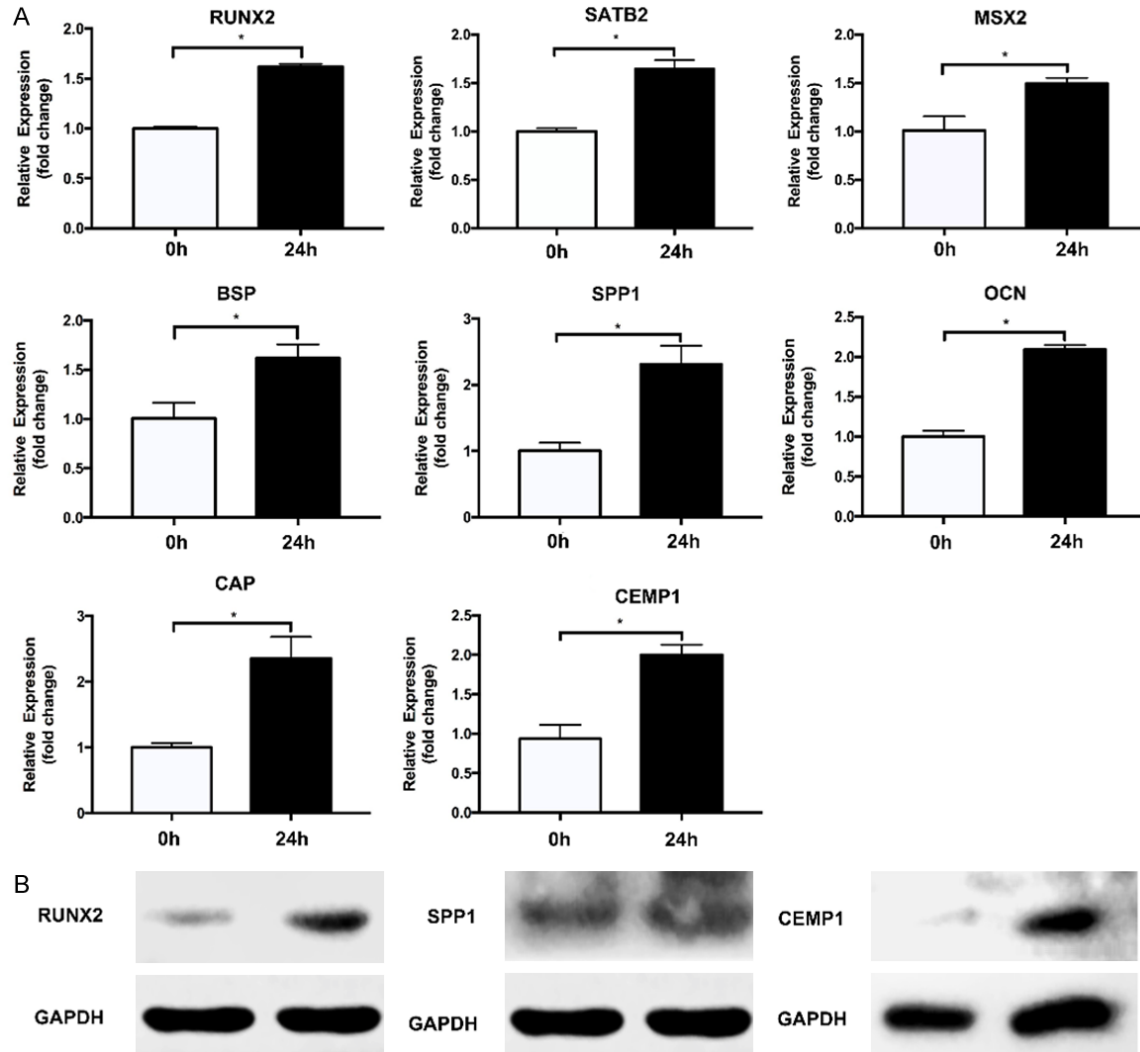


Figure 2. Effect of mechanical stretch on osteogenic/cementoblastic differentiation of cultured human periodontal ligament cells (PDLs). A. The osteogenic/cementoblastic markers RUNX2, SATB2, MSX2, BSP, SPP1, OCN, CAP, and CEMP1 were detected by RT-qPCR analysis and were found to be upregulated in the tension group ($P < 0.05$). B. Western blot analysis revealed that stretched PDLs had higher expression levels of osteogenic/cementoblastic proteins. $*P < 0.05$ vs. control.

nodule formation in PDLs after osteogenic induction for 7 days and 21 days, respectively (**Figure 1C, 1D**). The relative expression of all osteogenic genes was increased during the process of PDL osteogenesis (**Figure 1F**). Moreover, staining with Oil Red O showed the formation of lipid clusters in cultured cells (**Figure 1E**). These results indicate that PDLs were of mesenchymal origin and had multi-differentiation potential.

Mechanical stretch-induced osteogenic/cementoblastic differentiation of PDLs

PDLs at a density of 1×10^5 were seeded onto a six-well plate with a flexible silicon membrane.

After mechanical loading for 24 h, the stretched cells showed a higher expression level of osteogenic/cementoblastic genes and proteins compared with the cells in the control group (**Figure 2A, 2B**). This indicates that the osteoblastic/cementoblastic differentiation of PDLs was increased when mechanical force was imposed. See the original Western blot images in [Figures S1](#) and [S2](#).

Differentially expressed miRNAs

To analyze the variance in miRNAs during mechanical force loading, we compared the known miRNA expressions between stretched and non-stretched PDLs to identify the differ-

miRNAs and osteoblastic/cementoblastic differentiation of PDLs

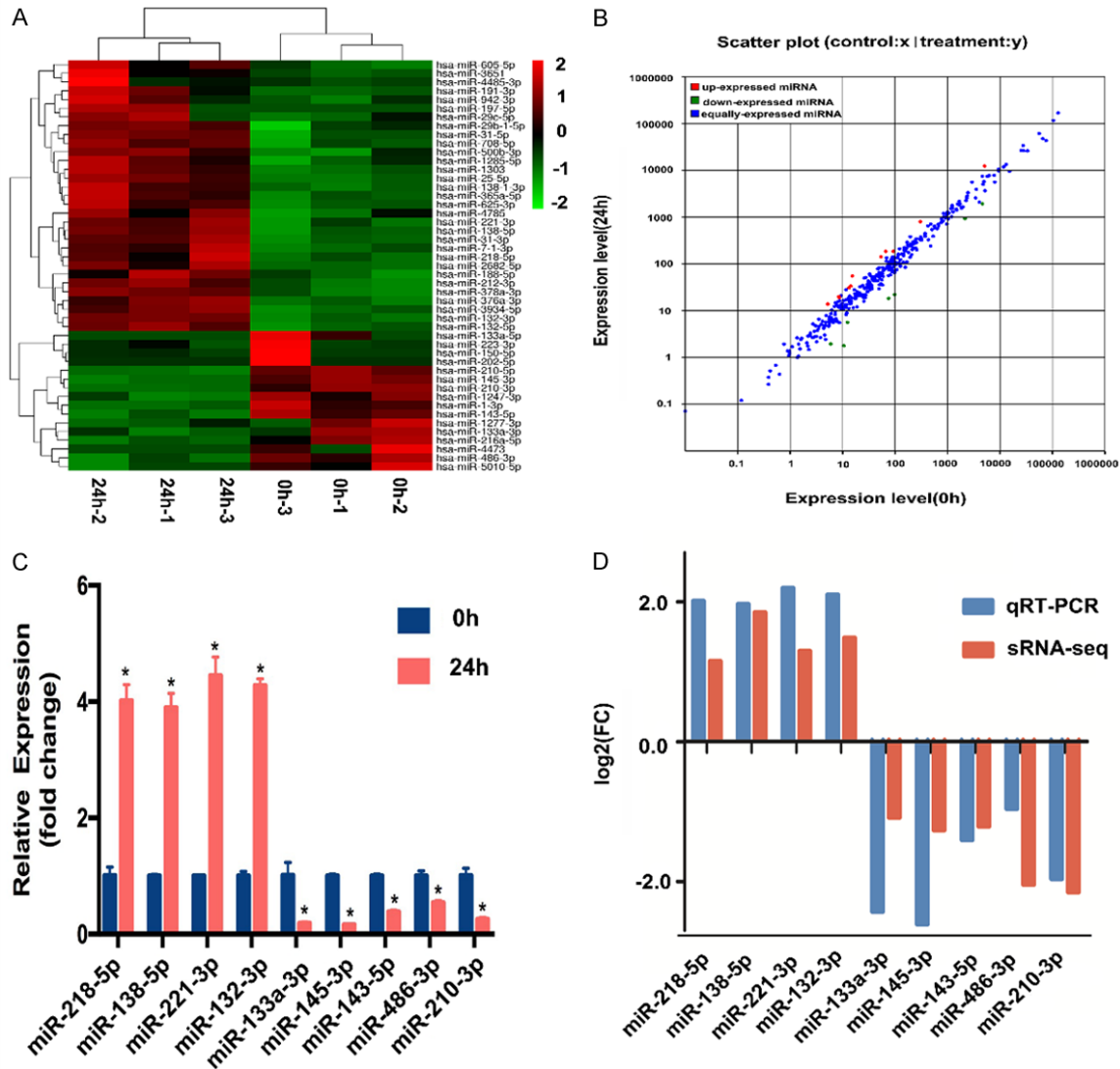


Figure 3. Hierarchical clustering analysis, scatter plot, and in vitro validation of differentially expressed miRNAs in stretched and non-stretched periodontal ligament cells (PDLs). (A) Cluster analysis of 47 differentially expressed miRNAs. Red color represents a relative high expression level. Green color shows a relative low expression level. In the stretched group, 31 miRNAs were significantly upregulated and 16 were downregulated compared with the control group. (B) miRNA scatter plot. Red dots represent significantly upregulated miRNAs in the stretched PDLs compared with the control cells. Green dots show significantly downregulated miRNAs. Blue dots represent equally-expressed miRNAs. (C) RT-qPCR was applied to verify the expression levels of differentially expressed miRNAs. Consistent with (D) the RNA-Seq results, miR-218-5p, miR-138-5p, miR-221-3p, and miR-132-3p were remarkably upregulated, while miR-133a-3p, miR-145-3p, miR-143-5p, miR-486-3p, and miR-210-3p were significantly downregulated in the stretched group ($P < 0.05$). * $P < 0.05$ vs. control.

entially expressed miRNAs. A heat map and cluster analysis was applied to visualize the miRNAs differentially expressed between the two groups. The analyses showed that 47 known miRNAs were differentially expressed, of which 31 were upregulated and 16 were downregulated in the stretched PDLs compared with the normal PDLs (Figure 3A). The overall distribution of the differentially expressed miRNAs is displayed in a scatter plot (Figure 3B).

Validation of differentially expressed miRNAs in vitro by RT-qPCR

To verify the results obtained from our RNA-Seq experiment, nine osteogenesis-related miRNAs were chosen for validation by RT-qPCR. The function and the validated osteogenesis-related targets of those nine miRNAs were reviewed according to the published literature by searching PubMed (Table S1). Consistent with the

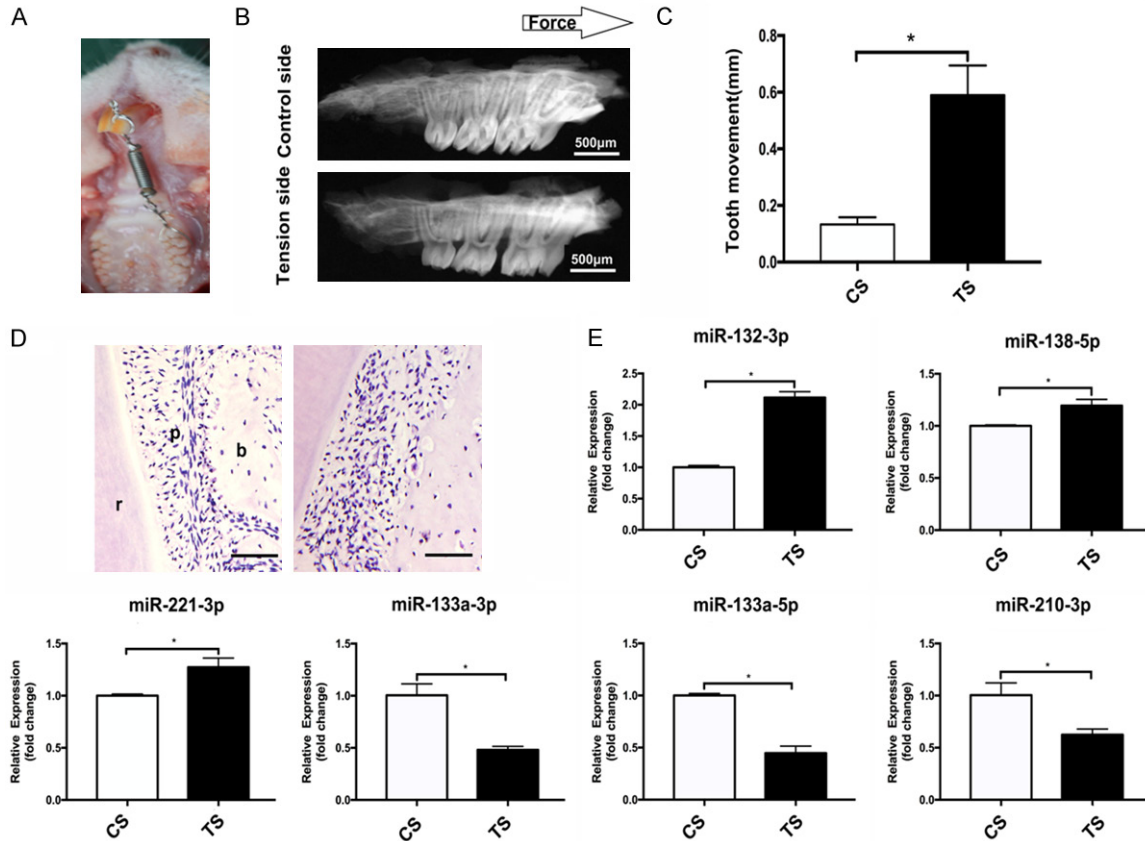


Figure 4. Rat orthodontic tooth movement (OTM) model and validation of differentially expressed miRNAs in vivo. A. A rat model for OTM. B. X-ray photography of orthodontic force induced tooth movement in rats after 14 days. Black arrow: force loading direction; scale bar: 500 μ m. C. Tooth movement measurement between cemento-enamel junctions of orthodontic loaded first molars and second molars for the tension force-stimulated site (TS) and the control site (CS). The results showed significantly more tooth movement in the tension site ($P < 0.05$). D. HE staining revealed more bone tissue volume in the stretched group (right) compared with the control group (left). Scale bar: 100 μ m; r: root; p: periodontium; b: alveolar bone. E. Six conserved miRNAs, including miR-221-3p, miR-138-5p, miR-132-3p, miR-210-3p, miR-133a-3p, and miR-133a-5p, were detected by RT-qPCR analysis. The results were consistent with our RNA-Seq and in vitro experiment ($P < 0.05$). * $P < 0.05$ vs. control.

RNA-Seq results, miR-218-5p, miR-138-5p, miR-221-3p, and miR-132-3p were remarkably upregulated, while miR-133a-3p, miR-145-3p, miR-143-5p, miR-486-3p, and miR-210-3p were significantly downregulated in the stretched group (Figure 3C, 3D). These results indicated that mechanical force could induce changes in the expression profile of miRNAs in PDLs.

Validation of miRNA expression in rats

To further confirm the expression levels of several conserved miRNAs after mechanical force loading, we established a rat model for OTM (Figure 4A). X-ray photographs and quantitative analysis (Figure 4B, 4C) indicated that OTM was evident after 14 days of force application at the maxillary first molar. HE staining revealed

that there was more bone tissue formation at the tension site compared with the control site (Figure 4D). Next, we isolated PDL tissue from both the stretched site and the control site after 3 days of orthodontic force loading. RT-qPCR was performed to detect the expression levels of six conserved miRNAs, including miR-221-3p, miR-138-5p, miR-132-3p, miR-210-3p, miR-133a-3p, and miR-133a-5p. The results were consistent with our RNA-Seq and in vitro experiment (Figure 4E).

Identification of differentially expressed miRNAs controlled by osteoblast-specific transcription factors

RUNX2, osterix (OSX), SATB2, MSX2, and DLX5 are well-known transcription factors that play a

Table 2. Osteogenesis-related transcription factor targeted by differentially expressed miRNAs

Transcription factor	Function	miRNA
RUNX2	Osteogenesis	miR-218-5p, miR-625-3p, miR-150-5p, miR-2682-5p, miR-7-1-3p, miR-221-3p, miR-133a-5p
Osterix	Osteogenesis	miR-486-3p, miR-145-3p, miR-143-5p, miR-133a-3p
SATB2	Osteogenesis	miR-218-5p, miR-1-3p, miR-31-5p, miR-376a-3p
MSX2	Osteogenesis	miR-7-1-3p, miR-708-5p, miR-942-3p
DLX5	Osteogenesis	miR-376a-3p, miR-942-3p

vital role in osteogenic differentiation. In the present study, the expressions of RUNX2, SATB2, and MSX2 were upregulated in PDLCs after mechanical loading (**Figure 2A**). In order to verify the regulatory effect of miRNAs on these transcription factors, we used three software programs to search for miRNA targeted osteogenesis-related transcription factors. As shown in **Table 2**, several miRNAs were predicted to target the above-mentioned transcription factors.

Functional analysis of mechanical stretch-responsive miRNAs

GO is an international standardized gene function classification system that comprehensively describes the properties of genes. To explore the potential functions of differentially expressed miRNAs in stretched PDLCs, we performed GO enrichment analysis to identify the functions significantly associated with the predicted target genes of the changed miRNAs. The most enriched GO terms in the biological process, cellular component, and molecular function domains are shown in **Figure 5A**.

KEGG analysis can identify the main pathways in which the target gene candidates of the changed miRNAs could be involved. The top 20 enriched pathways of the target genes are displayed in **Figure 5B**. Among them, the MAPK signaling pathway, cAMP signaling pathway, and Hippo signaling pathway were found to be involved in the regulation of osteogenesis.

Hippo signaling pathway is differentially expressed in stretched and non-stretched PDLCs

The Hippo signaling pathway is involved in mechano-transduction and osteogenesis. According to our RNA-Seq results, the Hippo signaling pathway was obviously enriched in biological function analysis of target genes associated with differentially expressed miRNAs. Furth-

ermore, several key components of the Hippo signaling pathway, such as YAP1, WWTR1, TEAD2, CTGF, DVL2, GDF5, GLI2, LIMD1, WTIP, LATS1, and TEAD1, were predicted to be target genes of the differentially expressed miRNAs (**Figure 6A**); the upregulation of these components in PDLCs submitted to mechanical force loading was validated by RT-qPCR (**Figure 6B**). Among them, YAP1, WWTR1, TEAD2, CTGF, DVL2, and GDF5 were found to be positive regulators of osteogenesis.

Discussion

OTM can be induced by the constant application of orthodontic force. PDL and alveolar bone cells can perceive and transfer the mechanical force into molecular events. As a result, bone formation and resorption occur at the tension and compressive sites, respectively. To date, the underlying mechanisms in this process have not been fully elucidated. In our study, we first developed an in vitro force-loading model for PDLCs to mimic the process of OTM. Then, we applied high-throughput sequencing to determine the expression profile of miRNAs in stretched and non-stretched PDLCs. We also performed prediction and functional analysis of target genes. Our findings suggest that multiple miRNAs may be involved in mechanical force-induced osteoblastic/cementoblastic differentiation of PDLCs.

A number of in vitro studies have demonstrated that PDLCs are mechanosensitive. Cyclic stretch can induce several biological changes in PDLCs, such as cell realignment, cytoskeleton organization, apoptosis, and angiogenesis [21-24]. In addition, previous studies have also reported that cyclic tension can promote the osteogenic differentiation of PDLCs. An in vitro study showed that cyclic tension resulted in increased osteogenic gene expression of PDLCs [25]. Another study reported that mechanical loading may control osteoblastic/cemento-

miRNAs and osteoblastic/cementoblastic differentiation of PDLCs

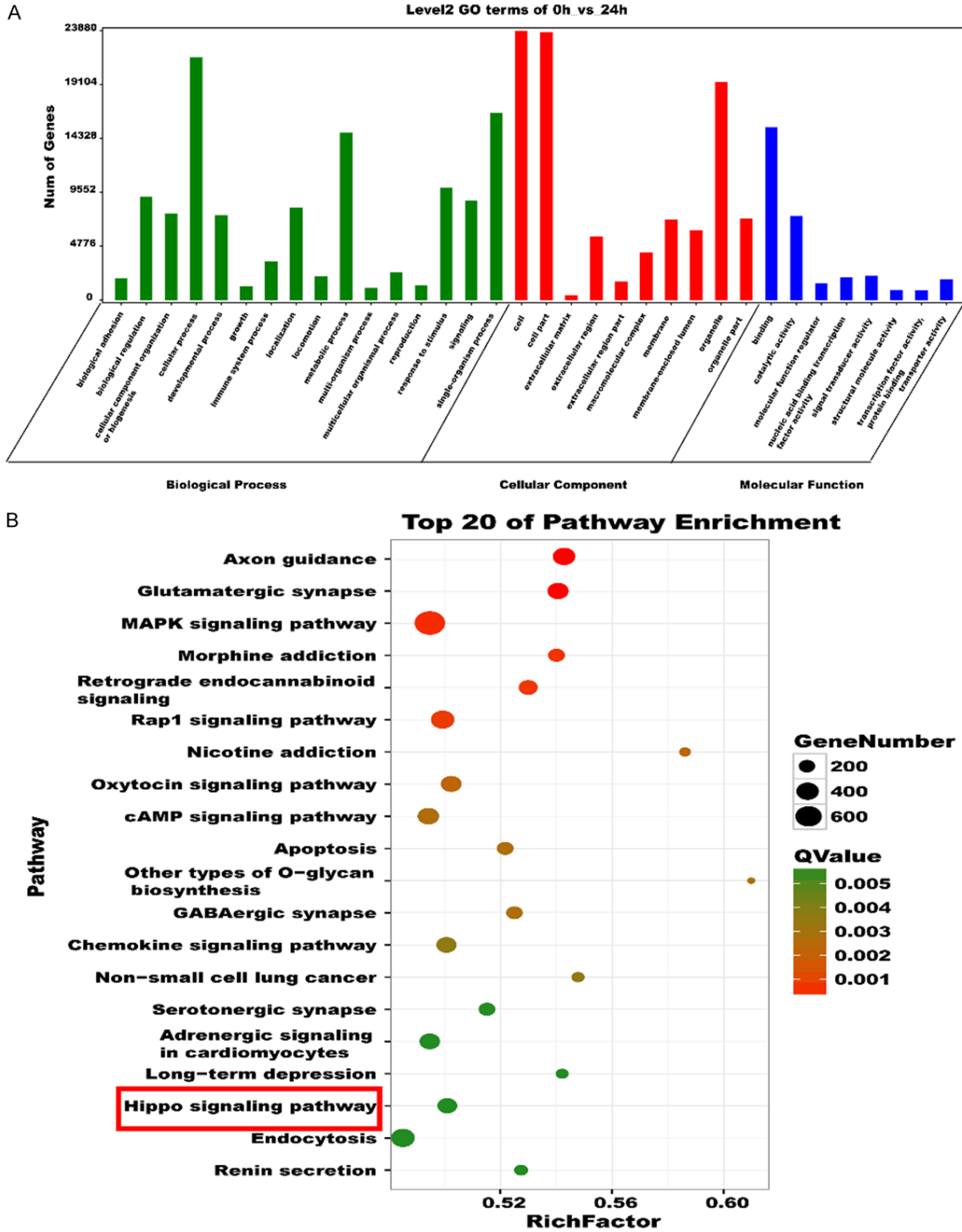


Figure 5. Functional analysis of mechanical stretch-responsive miRNAs. A. GO enrichment analysis indicated that target genes of differentially expressed miRNAs had a broad range of functions, including biological process, cellular components, and molecular function. B. Top 20 enriched pathways are shown in the scatter plot. The horizontal axis represents rich factor. The vertical axis shows the specific 20 enriched pathways.

blastic differentiation of PDLCs mediated by angiotensin II signaling [10]. In this study, we

observed higher expression of osteoblastic/cementoblastic genes and proteins in PDLCs

miRNAs and osteoblastic/cementoblastic differentiation of PDLs

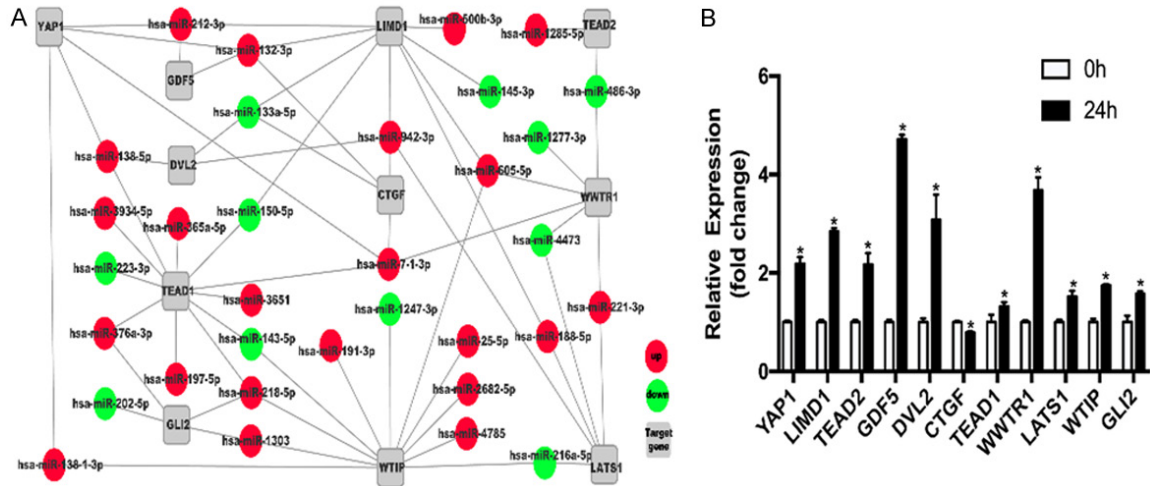


Figure 6. Differentially expressed miRNAs targeted core components of the Hippo signaling pathway. A. Regulatory networks of known differentially expressed miRNAs and the components of the Hippo signaling pathway. The red and green solid circles represent upregulated and downregulated miRNAs, respectively. The light grey box represents the components of the Hippo signaling pathway. B. RT-qPCR confirmed that the expression levels of several key components of the Hippo signaling pathway, including YAP1, WWTR1, TEAD2, CTGF, DVL2, GDF5, GLI2, LIMD1, WTIP, LATS1 and TEAD1, were upregulated in PDLs submitted to mechanical force loading ($P < 0.05$). * $P < 0.05$ vs. control.

after applying mechanical tension force loading, which was consistent with previous studies.

miRNAs are a type of small and non-coding RNA that regulate gene expression at the post-transcriptional level. Several previous studies have reported the expression profile of miRNAs in PDLs after force stimulation. One study detected the expression levels of miRNAs in PDLs treated with fluid shear stress using microRNA arrays [16]. Another study explored miRNA expression differences between normal PDLs and PDLs that underwent 72 hours of 12% cyclic tension force stimulation. The above study screened 3100 miRNAs, of which 17 miRNAs were upregulated and 15 miRNAs were downregulated [26]. In our study, we cultured PDLs under 10% equibiaxial strain at 0.1 Hz for 24 hours, and applied high-throughput sequencing to identify the expression profile of miRNAs. According to our results, the expression levels of 47 miRNAs were found to be altered after stretching, of which with 31 were upregulated and 16 were downregulated. The differences in results obtained by other scholars compared to our results may be attributed primarily to the analytical methods. Compared with microarray analysis, high-throughput sequencing can identify new miRNAs that have previously been unreported, including those

evident at low expression levels. Additionally, the effect of mechanical stimulation on cells may be related to the device, magnitude, duration, and frequency. Next, we selected nine osteogenesis-related miRNAs to be further validated by RT-qPCR. The results of our RT-qPCR analysis were consistent with the RNA-Seq experiment. The relative function and validated targets of those nine miRNAs in the process of osteogenesis were also reviewed in this study (see [Table S1](#)). However, further studies must be performed to determine whether these osteo-miRNAs are also involved in the process of osteogenic/cementoblastic differentiation of stretched PDLs.

Osteogenesis is a well-organized process involving various factors. In recent years, transcription factors have been found to combine with miRNAs to regulate osteogenic differentiation of MSCs. RUNX2, an early and primary osteogenic transcription factor, is responsible for the activation of osteoblast marker genes, including collagen type I alpha 1 chain (COL1A1), SPP1, and bone sialoprotein (BSP) [27]. Additionally, miR-133a was reported to be a key negative regulator of osteogenic differentiation of vascular smooth muscle cells, and this effect appeared to be mediated by targeting RUNX2 [28]. As a downstream gene of RUNX2, OSX is specifically expressed during osteoblast differ-

entiation and is critical for bone formation [29]. It has been shown that miR-143 and miR-145 can repress osteogenic differentiation through the regulation of OSX expression, forming a feedback loop with Kruppel-like factor 4 (KLF4) and OSX in odontoblasts [30]. DLX5 is a bone-inducing transcription factor that is expressed in the later stages of osteoblast differentiation [31]. A previous study showed that miR-203 and miR-320b can negatively regulate BMP2-induced osteoblast differentiation by suppressing DLX5, which in turn inhibits RUNX2 and OSX [32]. MSX2 has been found to act as an upstream factor of RUNX2 [33]. miRNA array analysis has revealed that miR-124a and miR-181a are important regulatory factors for osteoblastic differentiation of mouse-induced pluripotent stem cells; both can directly target DLX5 and MSX2 [34]. SATB2 is an important determinant of osteoblastic differentiation and can enhance the activity of RUNX2 and activate transcription factor 4 (ATF4) [35]. To date, several miRNAs have been reported to regulate osteoblastic differentiation by directly binding to the 3'-UTR of SATB2 mRNA [36, 37]. In summary, the above evidence suggests that regulation of transcription factors controlled by miRNAs is a crucial mechanism underlying osteogenic differentiation. In the present study, RUNX2, OSX, DLX5, MSX2, and SATB2 were predicted to be the targets for differentially expressed miRNAs in PDLs after force stimulation. Furthermore, the expression levels of RUNX2, MSX2, and SATB2 were found to be upregulated in tension force loading PDLs. Whether the differentially expressed miRNAs regulate the mechanical stretch-induced osteogenesis of PDLs by targeting these osteogenic specific transcription factors requires further study.

Increasing evidence indicates that the Hippo signaling pathway is regulated by mechanical stress. Several core components that are reported to be positive regulators of osteogenesis are involved in the Hippo signaling pathway. Yes-associated protein (YAP) and transcriptional coactivator with PDZ-binding motif (TAZ) are key downstream effectors of the Hippo signaling pathway, and have potential to function in mechano-transduction and osteogenic differentiation [38]. Cyclic stretch enhances the osteogenesis of PDLs via YAP-activation [39], and TAZ is indicated as a key mediator, promoting ADSC commitment to the osteoblast lineage [40]. TEA domain transcription factor 2 (TEAD2) is located in the nucleus, where it can

form a complex with YAP and co-activate the expression of multiple genes involved in cell fate determination, proliferation, and survival [41]. Connective tissue growth factor (CTGF) is a target gene of YAP; its expression is known to be induced by mechanical stimulation and is involved in osteogenic differentiation of mechanical stretched-associated ADSCs [42]. Growth differentiation factor 5 (GDF5) and Dishevelled 2 (DVL2) are another two components involved in the Hippo signaling pathway; they have been shown to be involved in the osteogenic differentiation of ligamentum flavum (LF)-derived stem cells (LFSCs) and synovial fibroblasts, respectively [43, 44]. Recently, a number of studies have demonstrated an association between miRNA and the Hippo signaling pathway during osteogenesis of human MSCs (hMSCs). One study showed that miR-135b-5p positively regulates osteogenic differentiation of hMSCs by controlling the expression levels of LATS1 and MOB1B, key negative regulators of the Hippo signaling pathway, resulting in subsequent activation of the Hippo signaling pathway [45]. In our study, YAP1, WWTR1, TEAD2, CTGF, DVL2, GDF5, GLI2, LIMD1, WTIP, LATS1, and TEAD1 were determined to be the target genes of differentially expressed miRNAs, and also were confirmed to be upregulated in stretched PDLs. Therefore, we speculate that the changed miRNAs can regulate the mechanical stretch-induced osteogenic/cementoblastic differentiation of PDLs via components of the Hippo signaling pathway.

In conclusion, we first identified and characterized the expression profile of miRNAs in PDLs after mechanical force loading using high-throughput sequencing. Furthermore, we explored a regulatory network between differentially expressed miRNAs and transcription factors to identify the potential mechanisms underlying osteogenic/cementoblastic differentiation of stretched PDLs. This study provides a basis for further insight into the molecular mechanisms involved in bone remodeling during OTM.

Acknowledgements

This work was financially supported by the National Natural Science Foundation of China (No. 81500888 and 81571011), the Youth Medical Experts' Project of Wuhan, Research Fund for the Doctoral Program of Higher Education (20120141130009) and Wuhan Applied Basic Research Project (No. 20160601010-

1004). We are very thankful for the technical assistance and bioinformatics analysis provided by Gene Denovo.

Disclosure of conflict of interest

None.

Address correspondence to: Shanshan Liang and Yining Wang, The State Key Laboratory Breeding Base of Basic Science of Stomatology (Hubei-MOST) and The Key Laboratory of Oral Biomedicine Ministry of Education, School and Hospital of Stomatology, Wuhan University, Wuhan, PR China. E-mail: wb000867@whu.edu.cn (SSL); wang.yn@whu.edu.cn (YNW)

References

[1] Beertsen W, McCulloch CA and Sodek J. The periodontal ligament: a unique, multifunctional connective tissue. *Periodontol* 2000 1997; 13: 20-40.

[2] Masella RS and Meister M. Current concepts in the biology of orthodontic tooth movement. *Am J Orthod Dentofacial Orthop* 2006; 129: 458-468.

[3] Wise GE and King GJ. Mechanisms of tooth eruption and orthodontic tooth movement. *J Dent Res* 2008; 87: 414-434.

[4] Kitaura H, Kimura K, Ishida M, Sugisawa H, Kohara H, Yoshimatsu M and Takano-Yamamoto T. Effect of cytokines on osteoclast formation and bone resorption during mechanical force loading of the periodontal membrane. *ScientificWorldJournal* 2014; 2014: 617032.

[5] Huang L, Liu B, Cha JY, Yuan G, Kelly M, Singh G, Hyman S, Brunski JB, Li J and Helms JA. Mechanoresponsive properties of the periodontal ligament. *J Dent Res* 2016; 95: 467-475.

[6] Baloul SS. Osteoclastogenesis and osteogenesis during tooth movement. *Front Oral Biol* 2016; 18: 75-79.

[7] Tsuge A, Noda K and Nakamura Y. Early tissue reaction in the tension zone of PDL during orthodontic tooth movement. *Arch Oral Biol* 2016; 65: 17-25.

[8] Diercke K, Kohl A, Lux CJ and Erber R. Strain-dependent up-regulation of ephrin-B2 protein in periodontal ligament fibroblasts contributes to osteogenesis during tooth movement. *J Biol Chem* 2011; 286: 37651-37664.

[9] Jiang L and Tang Z. Expression and regulation of the ERK1/2 and p38 MAPK signaling pathways in periodontal tissue remodeling of orthodontic tooth movement. *Mol Med Rep* 2018; 17: 1499-1506.

[10] Monnouchi S, Maeda H, Yuda A, Hamano S, Wada N, Tomokiyo A, Koori K, Sugii H, Serita S and Akamine A. Mechanical induction of interleukin-11 regulates osteoblastic/cementoblastic differentiation of human periodontal ligament stem/progenitor cells. *J Periodontol Res* 2015; 50: 231-239.

[11] Bartel DP. MicroRNAs: genomics, biogenesis, mechanism, and function. *Cell* 2004; 116: 281-297.

[12] Ghildiyal M and Zamore PD. Small silencing RNAs: an expanding universe. *Nat Rev Genet* 2009; 10: 94-108.

[13] Wang H, Sun Z, Wang Y, Hu Z, Zhou H, Zhang L, Hong B, Zhang S and Cao X. MiR-33-5p, a novel mechano-sensitive microRNA promotes osteoblast differentiation by targeting Hmga2. *Sci Rep* 2016; 6: 23170.

[14] Liu L, Liu M, Li R, Liu H, Du L, Chen H, Zhang Y, Zhang S and Liu D. MicroRNA-503-5p inhibits stretch-induced osteogenic differentiation and bone formation. *Cell Biol Int* 2017; 41: 112-123.

[15] Li J, Hu C, Han L, Liu L, Jing W, Tang W, Tian W and Long J. MiR-154-5p regulates osteogenic differentiation of adipose-derived mesenchymal stem cells under tensile stress through the Wnt/PCP pathway by targeting Wnt11. *Bone* 2015; 78: 130-141.

[16] Qi L and Zhang Y. The microRNA 132 regulates fluid shear stress-induced differentiation in periodontal ligament cells through mTOR signaling pathway. *Cell Physiol Biochem* 2014; 33: 433-445.

[17] Chen N, Sui BD, Hu CH, Cao J, Zheng CX, Hou R, Yang ZK, Zhao P, Chen Q, Yang QJ, Jin Y and Jin F. MicroRNA-21 contributes to orthodontic tooth movement. *J Dent Res* 2016; 95: 1425-1433.

[18] Wei F, Liu D, Feng C, Zhang F, Yang S, Hu Y, Ding G and Wang S. MicroRNA-21 mediates stretch-induced osteogenic differentiation in human periodontal ligament stem cells. *Stem Cells Dev* 2015; 24: 312-319.

[19] Chang M, Lin H, Fu H, Wang B, Han G and Fan M. MicroRNA-195-5p regulates osteogenic differentiation of periodontal ligament cells under mechanical loading. *J Cell Physiol* 2017; 232: 3762-3774.

[20] Behjati S and Tarpey PS. What is next generation sequencing? *Arch Dis Child Educ Pract Ed* 2013; 98: 236-238.

[21] Ma J, Zhao D, Wu Y, Xu C and Zhang F. Cyclic stretch induced gene expression of extracellular matrix and adhesion molecules in human periodontal ligament cells. *Arch Oral Biol* 2015; 60: 447-455.

[22] Zhao D, Wu Y, Xu C and Zhang F. Cyclic-stretch induces apoptosis in human periodontal liga-

miRNAs and osteoblastic/cementoblastic differentiation of PDLCs

- ment cells by activation of caspase-5. *Arch Oral Biol* 2017; 73: 129-135.
- [23] Wang YF, Zuo ZH, Luo P, Pang FS and Hu JT. The effect of cyclic tensile force on the actin cytoskeleton organization and morphology of human periodontal ligament cells. *Biochem Biophys Res Commun* 2018; 506: 950-955.
- [24] Narimiya T, Wada S, Kanzaki H, Ishikawa M, Tsuge A, Yamaguchi Y and Nakamura Y. Orthodontic tensile strain induces angiogenesis via type IV collagen degradation by matrix metalloproteinase-12. *J Periodontol Res* 2017; 52: 842-852.
- [25] Wescott DC, Pinkerton MN, Gaffey BJ, Beggs KT, Milne TJ and Meikle MC. Osteogenic gene expression by human periodontal ligament cells under cyclic tension. *J Dent Res* 2007; 86: 1212-1216.
- [26] Chang M, Lin H, Luo M, Wang J and Han G. Integrated miRNA and mRNA expression profiling of tension force-induced bone formation in periodontal ligament cells. *In Vitro Cell Dev Biol Anim* 2015; 51: 797-807.
- [27] Bruderer M, Richards RG, Alini M and Stoddart MJ. Role and regulation of RUNX2 in osteogenesis. *Eur Cell Mater* 2014; 28: 269-286.
- [28] Zhang Y, Xie RL, Croce CM, Stein JL, Lian JB, van Wijnen AJ and Stein GS. A program of microRNAs controls osteogenic lineage progression by targeting transcription factor RUNX2. *Proc Natl Acad Sci U S A* 2011; 108: 9863-9868.
- [29] Liu TM and Lee EH. Transcriptional regulatory cascades in RUNX2-dependent bone development. *Tissue Eng Part B Rev* 2013; 19: 254-263.
- [30] Liu H, Lin H, Zhang L, Sun Q, Yuan G, Zhang L, Chen S and Chen Z. MiR-145 and miR-143 regulate odontoblast differentiation through targeting *klf4* and *osx* genes in a feedback loop. *J Biol Chem* 2013; 288: 9261-9271.
- [31] Heo JS, Lee SG and Kim HO. Distal-less homeobox 5 is a master regulator of the osteogenesis of human mesenchymal stem cells. *Int J Mol Med* 2017; 40: 1486-1494.
- [32] Laxman N, Mallmin H, Nilsson O and Kindmark A. MiR-203 and miR-320 regulate bone morphogenetic protein-2-induced osteoblast differentiation by targeting distal-less homeobox 5 (*DLX5*). *Genes (Basel)* 2016; 8: E4.
- [33] Alappat S, Zhang ZY and Chen YP. *Msx* homeobox gene family and craniofacial development. *Cell Res* 2003; 13: 429-442.
- [34] Okamoto H, Matsumi Y, Hoshikawa Y, Takubo K, Ryoike K and Shiota G. Involvement of microRNAs in regulation of osteoblastic differentiation in mouse induced pluripotent stem cells. *PLoS One* 2012; 7: e43800.
- [35] Dobрева G, Chahrouh M, Dautzenberg M, Chirivella L, Kanzler B, Farinas I, Karsenty G and Grosschedl R. *SATB2* is a multifunctional determinant of craniofacial patterning and osteoblast differentiation. *Cell* 2006; 125: 971-986.
- [36] Tang J, Zhang Z, Jin X and Shi H. MiR-383 negatively regulates osteoblastic differentiation of bone marrow mesenchymal stem cells in rats by targeting *Satb2*. *Bone* 2018; 114: 137-143.
- [37] Hu N, Feng C, Jiang Y, Miao Q and Liu H. Regulatory effect of miR-205 on osteogenic differentiation of bone mesenchymal stem cells (BMSCs): possible role of *SATB2/RUNX2* and *ERK/MAPK* pathway. *Int J Mol Sci* 2015; 16: 10491-10506.
- [38] Ishihara E and Nishina H. Role of Hippo-YAP/TAZ signaling pathway in mechanotransduction. *Clin Calcium* 2016; 26: 1751-1756.
- [39] Yang Y, Wang BK, Chang ML, Wan ZQ and Han GL. Cyclic stretch enhances osteogenic differentiation of human periodontal ligament cells via YAP activation. *Biomed Res Int* 2018; 2018: 2174824.
- [40] Zhu Y, Wu Y, Cheng J, Wang Q, Li Z, Wang Y, Wang D, Wang H, Zhang W, Ye J, Jiang H and Wang L. Pharmacological activation of TAZ enhances osteogenic differentiation and bone formation of adipose-derived stem cells. *Stem Cell Res Ther* 2018; 9: 53.
- [41] Noland CL, Gierke S, Schnier PD, Murray J, Sandoval WN, Sagolla M, Dey A, Hannoush RN, Fairbrother WJ and Cunningham CN. Palmitoylation of TEAD transcription factors is required for their stability and function in Hippo pathway signaling. *Structure* 2016; 24: 179-186.
- [42] Xu Y, Wagner DR, Bekerman E, Chiou M, James AW, Carter D and Longaker MT. Connective tissue growth factor in regulation of RhoA mediated cytoskeletal tension associated osteogenesis of mouse adipose-derived stromal cells. *PLoS One* 2010; 5: e11279.
- [43] Qu X, Chen Z, Fan D, Sun C and Zeng Y. MiR-132-3p regulates the osteogenic differentiation of thoracic ligamentum flavum cells by inhibiting multiple osteogenesis-related genes. *Int J Mol Sci* 2016; 17: 1370.
- [44] Zhang L, Luan L and Ma Y. Dishevelled 2 modulates osteogenic differentiation of human synovial fibroblasts in osteoarthritis. *Mol Med Rep* 2018; 18: 292-298.
- [45] Si YJ, Ren QH, Bi L. MiR-135b-5p regulates human mesenchymal stem cell osteogenic differentiation by facilitating the Hippo signaling pathway. *Int J Clin Exp Med* 2017; 10: 7767-7775.

miRNAs and osteoblastic/cementoblastic differentiation of PDLs

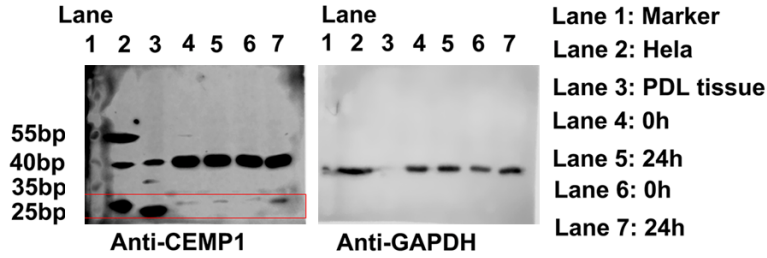


Figure S1. Western blot analysis of cementoblastic marker. Each protein lysate was loaded on SDS-PAGE gel as above order. HeLa cell line and periodontal ligament (PDL) tissue were used as positive control of CEMP1 expression, and GAPDH was used as internal control. The red box represents the location of CEMP1. Protein bands were detected by using an enhanced chemiluminescence (ECL) kit (Biosharp, Hefei, China) and visualized by Odyssey® CLx imaging system (LI-COR Biotechnology, Lincoln, NE, United States). The observed molecular weight of CEMP1 and GAPDH was 26 kDa and 37 kDa, respectively.

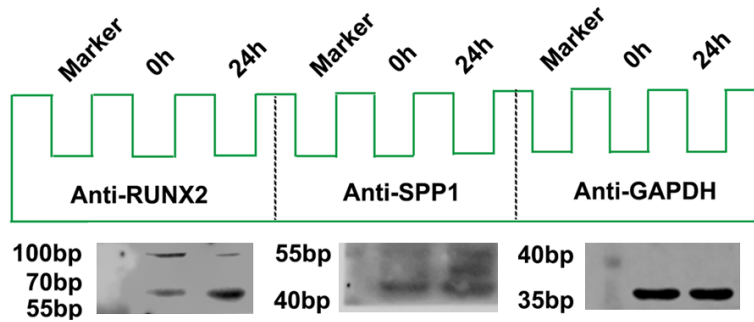


Figure S2. Western blot analysis of relative osteogenic proteins. Each protein sample was loaded on a 10% SDS-PAGE gel as above order, and transferred onto 0.22- μ m polyvinylidene difluoride (PVDF) membranes. The membranes were blocked with 5% non-fat milk for 1 h at room temperature. Then, these membranes were cut off at the dotted line and incubated with primary antibodies against human RUNX2, SPP1, and GAPDH at 4 °C overnight. Protein bands were detected by using an enhanced chemiluminescence (ECL) kit (Biosharp, Hefei, China) and visualized by Odyssey® CLx imaging system (LI-COR Biotechnology, Lincoln, NE, United States). The observed molecular weight of RUNX2, SPP1 and GAPDH was 70 kDa, 42 kDa and 37 kDa, respectively.

miRNAs and osteoblastic/cementoblastic differentiation of PDLCs

Table S1. Biological functions of selected miRNAs which are involved in osteoblastic differentiation

miRNAs	Validated targets	Cell lines	Biological function (osteogenesis: +; inhibit of osteogenesis: -)
1. miR-132-3p	1. FOXO1/GDF5/SOX6	1. Ligamentum flavum cells	1. - [1]
2. miR-132-3p	2. Ep300	2. Primary rat osteoblasts	2. - [2]
3. miR-132	3. Sirt1	3. MC3T3-E1 cells	3. - [3]
4. miR-132	4. β -catenin	4. Umbilical cord mesenchymal stem cells	4. - [4]
1. miR-221	1. RUNX2	1. C2C12 cells	1. - [5]
2. miR-221	2. ZFPM2	2. MC3T3-E1 cells	2. + [6]
1. miR-138	1. TRPS1/SULF2	1. 5TGM1	1. - [7]
2. miR-138	2. ZEB2	2. Human bone marrow mesenchymal stem cells (hBMSCs)	2. - [8]
3. miR-138-5p	3. EIF4EBP1	3. MC3T3-E1	3. - [9]
4. miR-138	4. FAK (PTK2)	4. BMSCs/Tendon-derived stem cells/Adipose-derived stem cells (ADSCs)	4. - [10]
5. miR-138-5p	5. Osteocalcin (OC)	5. Periodontal ligament stem cells	5. - [11]
1. miR-218	1. SFRP2/DKK2	1. hADSCs	1. + [12]
2. miR-218	2. RUNX2	2. Human dental stem cells	2. - [13]
3. miR-218	3. SOST/DKK2/SFRP2	3. BMSCs	3. + [14]
4. miR-218	4. TOB1	4. BMSCs	4. + [15]
5. miR-218	5. ROBO1	5. Fibroblast-like synovial cells	5. + [16]
1. miR-145	1. ZEB2	1. hBMSCs	1. - [8]
2. miR-145	2. Foxo1	2. hADSCs	2. - [17]
3. miR-145	3. Cbfb	3. MC3T3-E1	3. - [18]
4. miR-145	4. SP7	4. C2C12/MC3T3-E1	4. - [19]
1. miR-143	1. SP7	1. hBMSCs/MC3T3-E1	1. - [20]
2. miR-143-3p	2. RICTOR/LARP	2. hMSCs	2. - [21]
3. miR-143	3. TNF- α	3. Dental pulp stem cells	3. - [22]
1. miR-486	1. Smurf2	1. Aortic valve interstitial cells	1. + [23]
1. miR-133a-5p	1. RUNX2	1. MC3T3-E1	1. - [24]
2. miR-133a-3p	2. SLC39A1	2. BMSCs	2. - [25]
3. miR-133a	3. RUNX2	3. C2C12 cells/Vascular smooth muscle cells	3. - [26]
4. miR-133a	4. SP7	4. MC3T3	4. - [27]
5. miR-133a	5. RUNX2/TRPS1	5. C3H10T1/2/C2C12/NIH3T3/3T3-L1	5. - [28]
1. miR-210	1. EFNA3	1. hBMSCs	1. + [29]
2. miR-210-3p	2. SOST	2. BMSCs	2. + [30]
3. miR-210	3. ACVR1b	3. ST2 cells	3. + [31]

miRNAs and osteoblastic/cementoblastic differentiation of PDLs

References

- [1] Qu X, Chen Z, Fan D, Sun C and Zeng Y. MiR-132-3p regulates the osteogenic differentiation of thoracic ligamentum flavum cells by inhibiting multiple osteogenesis-related genes. *Int J Mol Sci* 2016; 17: 1370.
- [2] Hu Z, Wang Y, Sun Z, Wang H, Zhou H, Zhang L, Zhang S and Cao X. MiRNA-132-3p inhibits osteoblast differentiation by targeting Ep300 in simulated microgravity. *Sci Rep* 2015; 5: 18655.
- [3] Gong K, Qu B, Liao D, Liu D, Wang C, Zhou J and Pan X. MiR-132 regulates osteogenic differentiation via downregulating Sirtuin1 in a peroxisome proliferator-activated receptor beta/delta-dependent manner. *Biochem Biophys Res Commun* 2016; 478: 260-267.
- [4] Xue ZL, Meng YL and Ge JH. Upregulation of miR-132 attenuates osteoblast differentiation of UC-MSCs. *Eur Rev Med Pharmacol Sci* 2018; 22: 1580-1587.
- [5] Zhang Y, Gao Y, Cai L, Li F, Lou Y, Xu N, Kang Y and Yang H. MicroRNA-221 is involved in the regulation of osteoporosis through regulates RUNX2 protein expression and osteoblast differentiation. *Am J Transl Res* 2017; 9: 126-135.
- [6] Zheng X, Dai J, Zhang H and Ge Z. MicroRNA-221 promotes cell proliferation, migration, and differentiation by regulation of ZFPM2 in osteoblasts. *Braz J Med Biol Res* 2018; 51: e7574.
- [7] Tsukamoto S, Lovendorf MB, Park J, Salem KZ, Reagan MR, Manier S, Zavidij O, Rahmat M, Huynh D, Takagi S, Kawano Y, Kokubun K, Thruce CA, Nagano K, Petri A, Roccaro AM, Capelletti M, Baron R, Kauppinen S and Ghoobrial IM. Inhibition of microRNA-138 enhances bone formation in multiple myeloma bone marrow niche. *Leukemia* 2018; 32: 1739-1750.
- [8] Feng L, Shi L, Lu YF, Wang B, Tang T, Fu WM, He W, Li G and Zhang JF. Linc-ROR promotes osteogenic differentiation of mesenchymal stem cells by functioning as a competing endogenous RNA for miR-138 and miR-145. *Mol Ther Nucleic Acids* 2018; 11: 345-353.
- [9] Sun T, Leung F and Lu WW. MiR-9-5p, miR-675-5p and miR-138-5p damages the strontium and LRP5-mediated skeletal cell proliferation, differentiation, and adhesion. *Int J Mol Sci* 2016; 17: 236.
- [10] Wu J, Zhao J, Sun L, Pan Y, Wang H and Zhang WB. Long non-coding RNA H19 mediates mechanical tension-induced osteogenesis of bone marrow mesenchymal stem cells via FAK by sponging miR-138. *Bone* 2018; 108: 62-70.
- [11] Zhou X, Luan X, Chen Z, Francis M, Gopinathan G, Li W, Lu X, Li S, Wu C and Diekwisch TG. MicroRNA-138 inhibits periodontal progenitor differentiation under inflammatory conditions. *J Dent Res* 2016; 95: 230-237.
- [12] Zhang WB, Zhong WJ and Wang L. A signal-amplification circuit between miR-218 and Wnt/beta-catenin signal promotes human adipose tissue-derived stem cells osteogenic differentiation. *Bone* 2014; 58: 59-66.
- [13] Gay I, Cavender A, Peto D, Sun Z, Speer A, Cao H and Amendt BA. Differentiation of human dental stem cells reveals a role for microRNA-218. *J Periodontal Res* 2014; 49: 110-120.
- [14] Hassan MQ, Maeda Y, Taipaleenmaki H, Zhang W, Jafferji M, Gordon JA, Li Z, Croce CM, van Wijnen AJ, Stein JL, Stein GS and Lian JB. MiR-218 directs a Wnt signaling circuit to promote differentiation of osteoblasts and osteomimicry of metastatic cancer cells. *J Biol Chem* 2012; 287: 42084-42092.
- [15] Gao Y, Zhang Y, Lu Y, Wang Y, Kou X, Lou Y and Kang Y. TOB1 deficiency enhances the effect of bone marrow-derived mesenchymal stem cells on tendon-bone healing in a rat rotator cuff repair model. *Cell Physiol Biochem* 2016; 38: 319-329.
- [16] Iwamoto N, Fukui S, Takatani A, Shimizu T, Umeda M, Nishino A, Igawa T, Koga T, Kawashiri SY, Ichinose K, Tmai M, Nakamura H, Origuchi T, Chiba K, Osaki M, Jungel A, Gay S and Kawakami A. Osteogenic differentiation of fibroblast-like synovial cells in rheumatoid arthritis is induced by microRNA-218 through a ROBO/Slit pathway. *Arthritis Res Ther* 2018; 20: 189.
- [17] Hao W, Liu H, Zhou L, Sun Y, Su H, Ni J, He T, Shi P and Wang X. MiR-145 regulates osteogenic differentiation of human adipose-derived mesenchymal stem cells through targeting FoxO1. *Exp Biol Med (Maywood)* 2018; 243: 386-393.
- [18] Fukuda T, Ochi H, Sunamura S, Haiden A, Bando W, Inose H, Okawa A, Asou Y and Takeda S. MicroRNA-145 regulates osteoblastic differentiation by targeting the transcription factor Cbfb. *FEBS Lett* 2015; 589: 3302-3308.
- [19] Jia J, Tian Q, Ling S, Liu Y, Yang S and Shao Z. MiR-145 suppresses osteogenic differentiation by targeting Sp7. *FEBS Lett* 2013; 587: 3027-3031.
- [20] Gao Y, Xiao F, Wang C, Wang C, Cui P, Zhang X and Chen X. Long noncoding RNA MALAT1 promotes osterix expression to regulate osteogenic differentiation by targeting miRNA-143 in human bone marrow-derived mesenchymal stem cells. *J Cell Biochem* 2018; 119: 6986-6996.
- [21] Frith JE, Kusuma GD, Carthew J, Li F, Cloonan N, Gomez GA and Cooper-White JJ. Mechanically-sensitive miRNAs bias human mesenchymal stem cell fate via mTOR signalling. *Nat Commun* 2018; 9: 257.
- [22] Zhang P, Yang W, Wang G and Li Y. MiR-143 suppresses the osteogenic differentiation of dental pulp stem cells by inactivation of NF-kappaB signaling pathway via targeting TNF-alpha. *Arch Oral Biol* 2018; 87: 172-179.

miRNAs and osteoblastic/cementoblastic differentiation of PDLCs

- [23] Song R, Fullerton DA, Ao L, Zhao KS, Reece TB, Cleveland JC Jr and Meng X. Altered microRNA expression is responsible for the pro-osteogenic phenotype of interstitial cells in calcified human aortic valves. *J Am Heart Assoc* 2017; 6: e005364.
- [24] Zhang Y, Xie RL, Croce CM, Stein JL, Lian JB, van Wijnen AJ and Stein GS. A program of microRNAs controls osteogenic lineage progression by targeting transcription factor RUNX2. *Proc Natl Acad Sci U S A* 2011; 108: 9863-9868.
- [25] Mencia Castano I, Curtin CM, Duffy GP and O'Brien FJ. Next generation bone tissue engineering: non-viral miR-133a inhibition using collagen-nanohydroxyapatite scaffolds rapidly enhances osteogenesis. *Sci Rep* 2016; 6: 27941.
- [26] Li Z, Hassan MQ, Volinia S, van Wijnen AJ, Stein JL, Croce CM, Lian JB and Stein GS. A microRNA signature for a BMP2-induced osteoblast lineage commitment program. *Proc Natl Acad Sci U S A* 2008; 105: 13906-13911.
- [27] Chen Q, Liu W, Sinha KM, Yasuda H and de Crombrughe B. Identification and characterization of microRNAs controlled by the osteoblast-specific transcription factor Osterix. *PLoS One* 2013; 8: e58104.
- [28] Zhang Y, Xie RL, Gordon J, LeBlanc K, Stein JL, Lian JB, van Wijnen AJ and Stein GS. Control of mesenchymal lineage progression by microRNAs targeting skeletal gene regulators Trps1 and RUNX2. *J Biol Chem* 2012; 287: 21926-21935.
- [29] Qiu Y, Chen Y, Zeng T, Guo W, Zhou W and Yang X. EGCG ameliorates the hypoxia-induced apoptosis and osteogenic differentiation reduction of mesenchymal stem cells via upregulating miR-210. *Mol Biol Rep* 2016; 43: 183-193.
- [30] Hu B, Li Y, Wang M, Zhu Y, Zhou Y, Sui B, Tan Y, Ning Y, Wang J, He J, Yang C and Zou D. Functional reconstruction of critical-sized load-bearing bone defects using a Sclerostin-targeting miR-210-3p-based construct to enhance osteogenic activity. *Acta Biomater* 2018; 76: 275-282.
- [31] Mizuno Y, Tokuzawa Y, Ninomiya Y, Yagi K, Yatsuka-Kanesaki Y, Suda T, Fukuda T, Katagiri T, Kondoh Y, Aemiyama T, Tashiro H and Okazaki Y. MiR-210 promotes osteoblastic differentiation through inhibition of AcvR1b. *FEBS Lett* 2009; 583: 2263-2268.